Full Scale and Model Scale Propeller Ventilation Behind Ship

Luca Savio[1], Silas Spence[1], Kourosh Koushan[1], Sverre Steen[2]

[1]Norwegian Marine Technology Research Institute (MARINTEK), Trondheim, Norway
[2]Department of Marine Technology, Norwegian University of Science and Technology (NTNU), Trondheim, Norway

ABSTRACT

In the present paper the results from several experimental campaigns aimed to better understand the phenomenon of propeller ventilation are presented. The paper includes both reanalysis of already published data and the analysis of new experimental data. The presented data were collected both in full scale and in model scale. The model scale data features propeller open water tests in the towing tank and free running model in calm water and in waves in the ocean basin. Both set of experiments were carried out in MARINTEK facilities. The full scale data were recorded by means of a ship propulsion monitoring system called HeMoS, developed by Rolls Royce Marine. The full scale data have been used as a basis for the tests in the ocean basin. This work was carried out in the framework of Era-Net Martec project PropSeas.

Keywords

Ventilation, propulsion, experimental hydrodynamics

1 INTRODUCTION

This paper summarizes the results obtained through the model scale and full scale experiments carried out in the framework of the Era-Net Martec project PropSeas. The main goal of the project was to understand the reason for the failure of the ship's propulsive unit due to the operation of the ship in extreme seas. Among the various dynamic effects the propulsive unit is exposed to in rough sea states, ventilation has always been considered to be one of the most dangerous. For this reason extensive research was devoted to finding the conditions which lead to extreme propeller loads due to ventilation. These kind of studies, from the experimental point of view, have previously been undertaken by studying the propeller alone, i.e. not being surrounded by the ship hull. This is of course an idealized case in which the propeller immersion can be controlled. In a more realistic scenario ventilation happens when the propeller comes close enough to the free surface, as a result of the ship motions, to draw air from the free surface. The fact that the propeller is operating behind a ship hull has the twofold effect on ventilation of partly blocking the access to the free surface and of phasing the events according to both ship motions and the incoming wave periods. During the previous tests, carried out with the propeller alone in calm water and in regular waves at different submergences, no large loads were recorded so it was decided to run tests in

the more realistic scenario of a propeller working behind a ship. In order to reproduce this more realistic scenario a series of tests have been performed in the MARINTEK ocean basin using a free running ship model. The tests included both calm water runs and irregular seas at different wave encounter angles. In addition to the model test data the project featured full scale in-service monitoring data.

In order to better understand the limitations of the tests carried out in the towing tank, it is useful to briefly summarize what has been found so far with this kind of tests. In Figure 1 the time series of blade thrust coefficient is plotted for a propeller working at a static immersion ratio (h/R) equal to 1.5 and at an advance coefficient (J) equal to 0.3. In the first part of the time series the ventilation is unstable, while the second part the blade is fully ventilated.
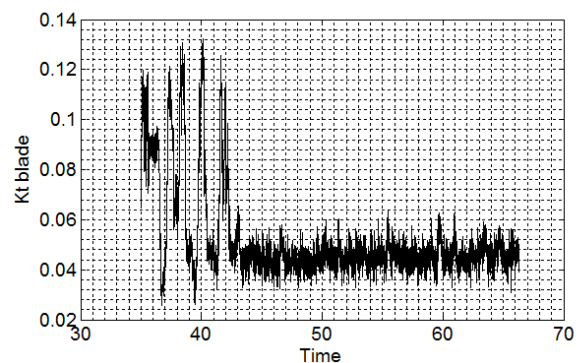

Figure 1 Time series of Kt blade versus time for a propeller subjcted to unstable ventilation in the towing tank.

During the unstable part of the time series the thrust coefficient is oscillating between the approximate value of the non-ventilated thrust coefficient to the fully ventilated one. By taking the first derivative of the thrust with respect to time it can be seen that the thrust drops more rapidly than it recovers. The first derivative of the thrust coefficient is shown in Figure 2. This highly dynamic scenario however does not lead to any large overload. The blade thrust or more generally any of the blade loads are varying considerably but always in the range which spans from the deeply submerged open water load to the fully ventilated one.
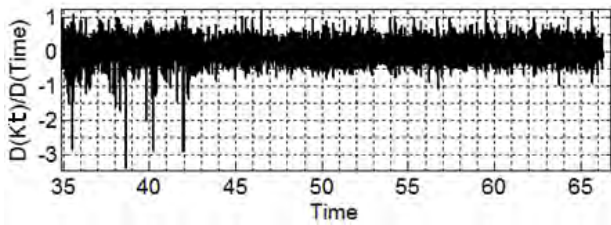
Figure 2 First time derivative of the blade Kt time series shown in Figure 1

The spread of the blade thrust coefficient is reported in Figure 3 by means of the distribution of the relative frequency of occurrence of the ratio between the blade thrust coefficient in ventilating and in open water non-ventilating condition. The distribution of the relative frequency of occurrence is calculated as follows. The range which encompasses all the observed values for a given variable is divided into intervals (which are called bins). The number of observed values which fall inside each bin is counted and then divided by the total number of samples. In Figure 3 the distribution is calculated only for the first part of the time series in order to focus on the unstable ventilation behavior. In Figure 3 it can be seen that the spread in the thrust coefficient is large, but also that values even slightly larger than the non-ventilating open water coefficient are seldom recorded.
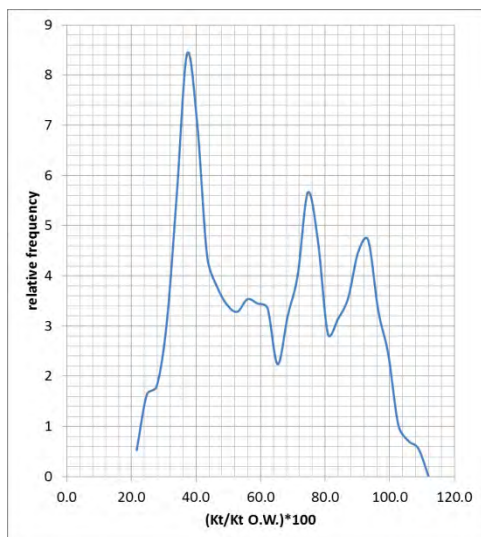

Figure 3 Blade Kt relative frequency of occurrence during unstable ventilation.

It is therefore unlikely that ventilation alone can produce large overloads. It can be argued that the large overloads can be extremely rare and therefore a single run is not really representative of the probability of large overloads to happen. However throughout the years a large number of experiments have been carried out, none of them showed large overloads. The fact that propeller/blade load can range from 0 to 100 percent of the open water value was reported also by Koushan (2006) and Koushan et al. (2009). In the tests performed by Koushan the propeller was subjected to heave motion from completely submerged to completely out of water (Koushan 2006) and to regular sinusoidal waves (Koushan et al. 2009). In both the above mentioned papers a large spread in propeller thrust and torque is reported, but always in the mentioned range from 0 to 100 percent. However in all the tests carried out so far, due to the fact that they have been carried out in open water condition, the dynamics of a propeller working behind a ship were not fully reproduced. The experiments detailed in the present paper aim to study how ventilation develops when the propeller is operating behind a ship.

The PropSeas project features also the opportunity of having access to full scale monitoring data, which are collected by the HeMoS system developed by Rolls Royce Marine. The HeMoS system is a health monitoring system for the propulsive system, which can be also used to improve the operation of the ship through a more rational use of its propulsive system. Such an advanced monitoring system can have many by-products. One of the first by-products identified was the possibility to identify ventilation events. This possibility was discovered by Leif Vartdal and Leif Aarseth of Rolls Royce Marine and further developed and presented by Savio and Steen (2012).

2 MODEL TESTS SPECIFICATIONS

The HeMoS system is currently installed on a supply vessel equipped with two azimuthing pulling thrusters. The model was a free running model equipped according to MARINTEK standard for sea-keeping and maneuvering tests. In addition to the standard equipment the model featured also a blade dynamometer mounted on the port propeller. Underwater cameras were fit to the hull in order to provide videos of the ventilation events. The change in model resistance due to the cameras was deemed to be minor compared to the added resistance due to the large waves the model was exposed to. In Figure 4 the model tested in the ocean basin is shown, whereas the data are reported in Table 1
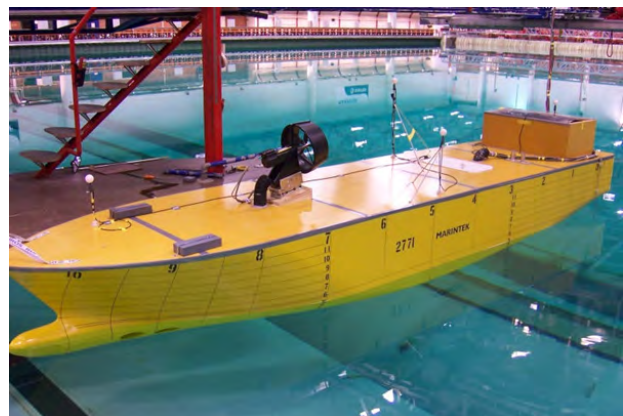

Figure 4 The tested model in the ocean basin

Table 1 Model data for the tests

Length between perpendiculars	5.05	[m]
Beam	1.313	[m]
Draft fp / ap	5.050/5.55	[m]
Displacement	1537.9	[kg]

The model was tested both in calm water and in waves. During the calm water runs standard maneuvers and ventilation specific tests were performed. The ventilation tests in calm water were performed by trimming the model bow down so that the propeller blade tip was touching the free surface. The tests in waves included both regular and irregular waves. The tests performed in irregular seas were designed to match the sea states and ship's wave encounter angles which statistically recorded more ventilation events according to the analysis of the full scale data performed by Savio and Steen (2012).

3 MODEL TESTS IN CALM WATER – NON VENTILATING CONDITION

The tests performed in calm water with the propeller in non-ventilating condition were meant to study the blade load when the ship is maneuvering. The model was ballasted to match the normal operational trim. The ship used for the tests is equipped with two azimuthing thrusters. The combination of ship maneuver and unit steering can lead to large in-plane velocity on the propeller disk. During the tests it was found that the in plane velocity can be large enough to produce blade thrust variations ranging from almost zero to 1.5 times the straight course Kt. In Figure 5 a zig-zag tests is presented. The performed maneuver was a standard 10-10 tests (Figure 5- bottom). In the top part of Figure 5 the thrust coefficient Kt for the blade is presented. The largest thrust oscillation are naturally found during the counter-steering phase (Figure 5 – center).
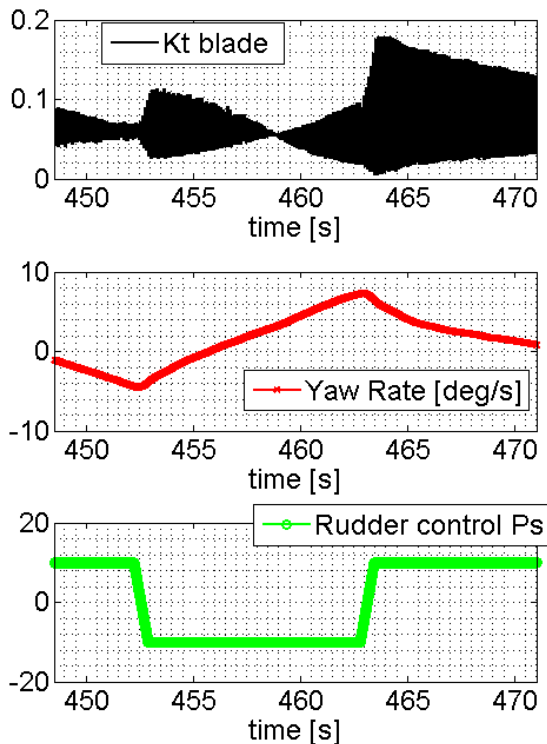
Figure 5 Data from a 10-10 zig zag maneuver in the ocean basin.

The Kt signal can be decomposed into two main components: a low frequency component arising from the model maneuvering and a blade passage component relative to the blade working in oblique inflow. The first component is retrieved by a low pass filter and plotted in Figure 6. The blade thrust coefficient is plotted relative to straight course blade thrust coefficient Kt0, in order to set a reference to a meaningful value.
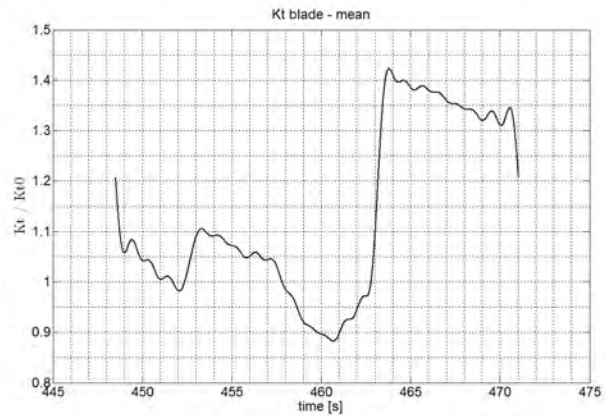
Figure 6 Low frequency component of the blade thrust during the zig-zag maneuver

The amplitude of the blade harmonic oscillation can be extracted by means of a band pass filter and an envelope detector, such as the Hilbert transform. The result is depicted in Figure 7, where it can be seen that the maximum amplitude of the oscillating component of the blade thrust is as high as 1.5 times the straight course blade thrust Kt0.
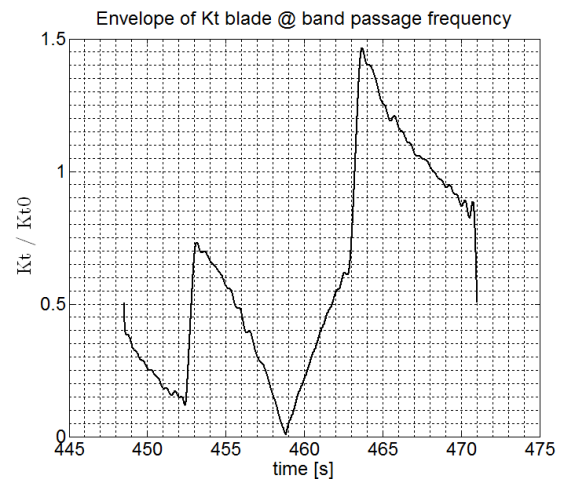
Figure 7 Blade passage frequency component of the blade thrust coefficient during the zig zag maneauver.

These large thrust oscillations could be amplified if the large angle of attack variations involved trigger for instance unstable sheet cavitation.

4 MODEL TESTS IN CALM WATER – VENTILATING CONDITION

A set of the tests were devoted to reproduce ventilation in a controlled scenario, which could also be reproduced during sea trials. The adopted strategy was to trim the model bow down until the propeller tip reached the free

surface in the upper part of the turn. The model was in full free running condition and was accelerated from rest simulating a slam start, including a scaled propeller revolution ramp. A typical run is presented in Figure 8. The propeller is experiencing all the ventilation condition from fully ventilating to non-ventilating condition. The transition between the fully ventilated to the non-ventilated conditions is marked by regime in which ventilation is unstable and in Figure 8 happens between 170 and 180 seconds approximately. This region of instability is where the largest dynamic effects are expected. However during the reported tests no large overloads have been recorded. Also when ventilation was unstable the blade thrust was varying from the fully ventilated value to the non-ventilating one, confirming what already observed in the tests with propeller alone in the towing tank.
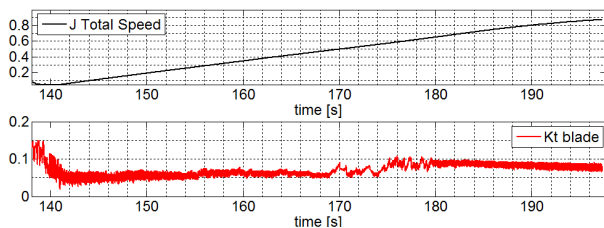

Figure 8 Trimmed (bow down) ventilation test, showing two distinct ventilation regimes separeted by a phase of unstable ventilation from time 170 to time 180.

The tests were performed with both units pointing straight forward (0 toe), with both units pointing inward (5 and 10 degrees toe in) and with both units pointing outwards (5 and 10 degrees toe out). The aim of these tests was to investigate the effect of the hull on ventilation. It is believed that the inception of ventilation is postponed when the propeller is pointing inwards because the hull is blocking the access of the propeller to the free surface. In order to partially confirm this hypothesis the free stream advance coefficient when the ventilation instability started and ended were recorded for the different toe angles. In Figure 9 the observed values are reported against the toe angle, which is set to be positive for toe in angles.
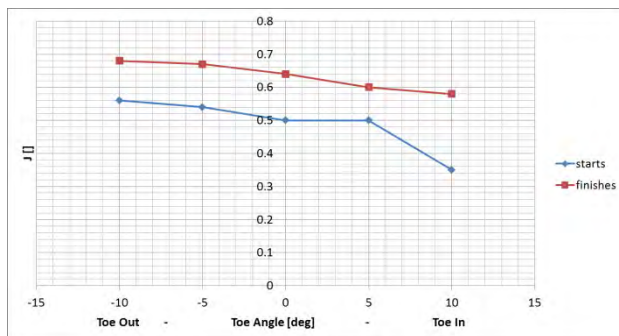

Figure 9 Effect of the unit toe on the inception and end advance coefficient of the unstable ventilation

Figure 9 shows that unstable ventilation occurs at lower J values when the units are pointing inwards; confirming at

least that the hull effect has to be taken into account when addressing ventilation in full scale.

5 MODEL TESTS IN IRREGULAR WAVES

A large part of the tests were devoted to study ventilation in the more realistic scenario of the ship model subjected to two different irregular wave spectra at different wave encounter angles. The tests matrix is given in Table 1.

Table 2 Wave spectral values (Jonswap spectrum) and wave headings applied in ocean basin tests

Parameter	Values (full scale)
Hs (m)	2, 4, 5
Period (s)	8.5, 10
Wave angle	30, 60, 120, 150

Since the major interest was to stimulate ventilation events rather than exposing the model to a given sea spectrum, the model was run just when the largest waves were generated. The wave angle is defined to be zero for the ship in head seas and to be counted positive in counterclockwise direction. Although this convention is not the usual sea-keeping convention, it will be adopted here because is the one adopted during the tests.

In order to detect an incipient ventilation event a pressure transducer was mounted on top of the propeller flush to the hull. The output of the pressure transducers reflects the submergence at that point and hence it is related to the ship motions relative to the incoming waves. When the signal from the pressure transducers becomes flat then the sensor is exposed to the atmospheric pressure and the chances that ventilation happens are high. The ventilation events were confirmed by means of the two cameras which have been placed on the ship keel slightly upstream of the propeller. A typical time series of model being subjected to some large waves is presented in Figure 10, where the blade thrust coefficient (top) is plotted together with the pressure transducers signal (center) and the unit rudder heading angle (bottom). It is interesting to note that when the pressure transducer became flat the blade thrust oscillations are reduced. On the contrary large blade thrust oscillations were observed in correspondence of large unit heading angles.
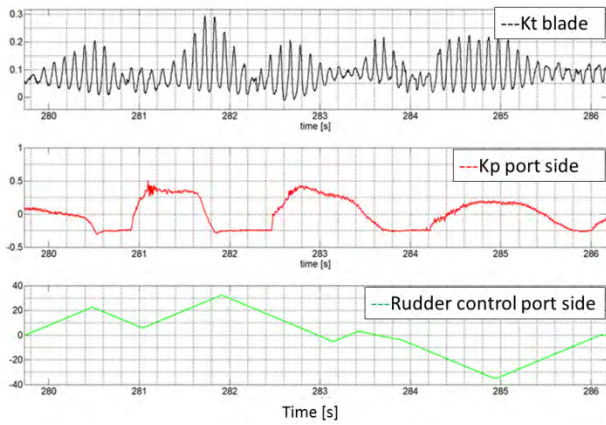
Figure 10 Time series of blade thrust coefficient, pressure coefficient and rudder control for the port unit.

The above reported event was recorded at 30 degrees wave angle, with a 5m significant height and 8.5 seconds spectrum. Another interesting event was recorded with the same wave spectrum but at 150 degrees wave angle. This event is reported in Figure 11, where the normalized values of Kt, Kp and rudder control angle are plotted on the same axes in order to ease the analysis of the event. Around time equal to 271 seconds the pressure sensor came in contact with the free surface. Slightly afterwards the blade thrust, which was showing large oscillation due to the large in-plane inflow generated by the steering of the unit (rudder control), suddenly dropped and the oscillation were reduced. The event terminated at second 271.6 approximately when the pressure transducer reentered into water. As soon as the ventilation event ends the large thrust oscillations due the unit steering reappear.
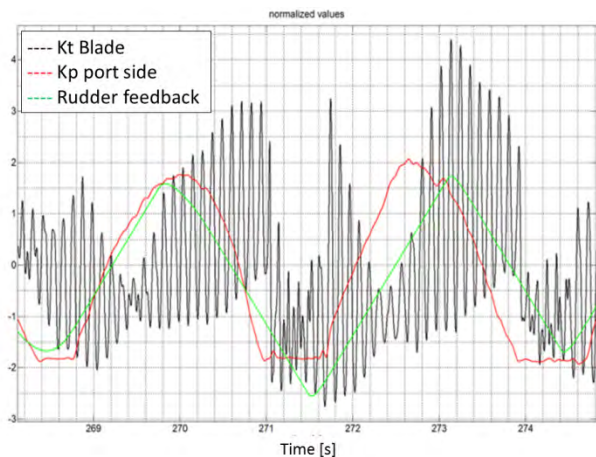

Figure 11 time series of of blade thruster coefficient, pressure coefficient and rudder control feedback.

The sudden drop in blade thrust is better highlighted by taking the first derivative versus time of the blade thrust as it shown in Figure 12, where the upper plot is the first derivative of the blade thrust coefficient and the lower plot the blade thrust coefficient time series reported for comparison. In Figure 12 it can be clearly seen that the thrust drop happened faster than the recovery, which happened around time 271.6 seconds.
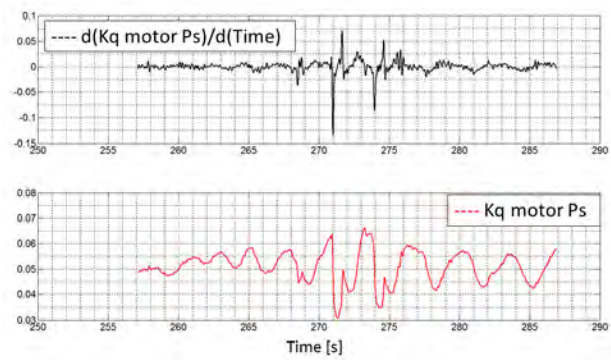

Figure 12 Blade thrust coefficient derivative (top) and Kt blade time series (bottom)

Since the pressure signal in Figure 11 shows that the air was present on top of the propeller for 0.6 seconds, which correspond to 5.4 propeller rotations at the propeller speed used during the experiments, it is expected that all the propeller blades were subjected to ventilation. The fact that all the blade were subject to ventilation is also confirmed by Figure 13, where the top figure is the first derivative of the propeller torque coefficient with respect to time and the bottom figure the propeller torque coefficient time series reported for reference. In order to allow for comparing with the full scale data the events are analyzed as follows. It has to be pointed out that only major events have been considered, which means that a significant and fast torque drop must be clearly visible in the data and not only in the video to be included among the events to be compared with the full scale data. For the events the torque drop and time elapsed from the start of the event to the minimum of the torque have been recorded.
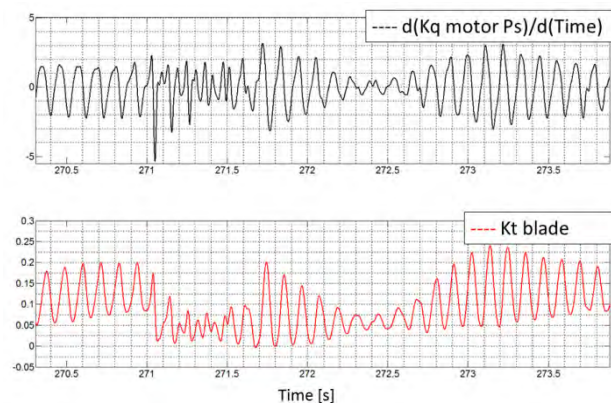

Figure 13 Propeller drive motor torque coefficient, first time derivative top and time series bottom

The model scale recorded events had an elapsed time from the start of the event to the end of the torque drop in the range from 0.2 seconds to 0.4 seconds and a typical torque coefficient drop in the range 0.011 to 0.033. The average torque coefficient decrease rates for the analyzed events were comprised between 0.055 and 0.10 Kq/s. The events statistics had as expected a correlation with the wave encounter angle. The events recorded during bow quartering seas were more violent in terms of torque decrease rate than the ones recorded at stern quartering seas. In Figure 14 the torque coefficient decrease rate is

plotted against the wave encounter angle. The events at bow quartering seas were more violent than the events at stern quartering seas probably because propeller ventilation on a ship is primary a ship motions related phenomenon.
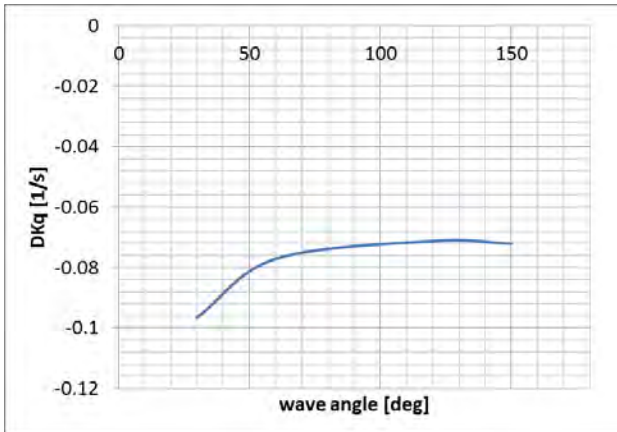

Figure 14 Torque coefficient decrease rate against wave encounter angle

In order to further stress the correlation between the violence of the events and the wave encounter angle the torque coefficient drops and the time duration of the torque are reported in Figure 15 against the wave encounter angle. From Figure 15 it can be seen that the events at stern quartering seas have a longer duration due to the slower ship motions, which leads to larger torque drops. However the larger torque drops develops over a longer time leading to a less violent event.
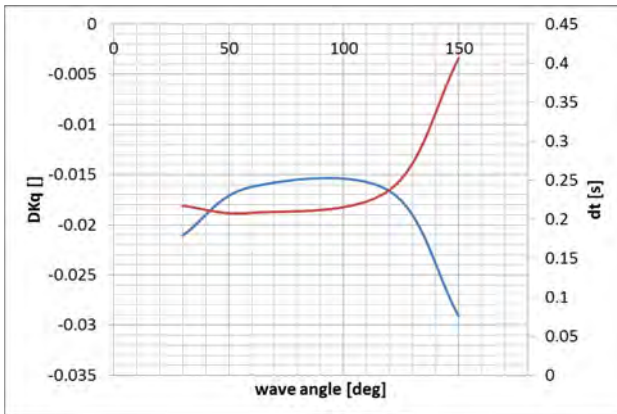

Figure 15 Torque coefficient drop (blue curve) and elapsed time (red curve) from the start of the event to the minimum of the torque coefficient

A more detailed analysis of the differences in the ventilation events in relation to the wave encounter angle is necessary to compare the model scale data with the full scale data. In the analysis presented before the pressure sensor mounted flush to the hull was used. However this sensor is not installed on the ship. Therefore for the sake of comparing the model scale data with the full scale data the submergence index was used. The submergence index is an approximate measure of how close the propeller might come close to the free surface on the basis of the ship motion. The submergence index for this vessel is defined as follows:

$$sub\ index = -3 * \tan(pitch) + sign * \tan(roll) \quad (1)$$

Where **pitch** and **roll** are the vessel pitch and roll angles respectively, and **sign** is equal to one if the port side unit is considered otherwise it is -1. The submergence index is zero for the vessel at an even keel and it is positive when the propeller under examination is moved above its even keel condition. In order to phase the ventilation events with the ship motions the time difference between the time when the minimum Kq occurred and the time when the maximum submergence index happened has been recorded and it is plotted in Figure 16. In Figure 16 a positive difference means that the propeller reached the top position before the torque reached the minimum. The clear trend in the data means that the wave angle has strong impact on the ventilation events. This impact can be both due to the different response of the ship but also due to the control system. The heading angle is controlled by the model autopilot, which in this case was the standard autopilot used in MARINTEK. The full scale autopilot is of course different and therefore reacts in a different way when the ship is subjected to the same sea state. Moreover it has to be remarked, although obvious, that the ship is also likely to be subjected to strong winds in the large sea states which were simulated in the model scale tests. The wind force on the model was neglected and hence the model scale autopilot did not have to counteract the action of wind.
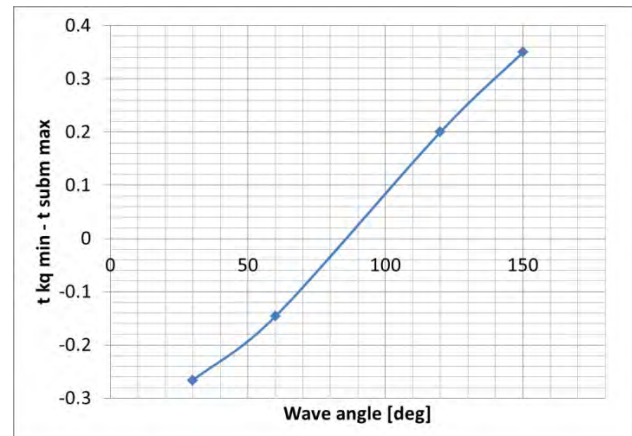

Figure 16 time difference between the maximum of the submergence index and the minimum of the torque coefficient.

During the experiment it was noted that the ventilation events occurred while the unit was pointing outwards with respect to the keel in stern quartering seas and inwards in bow quartering seas. The heading relation to the wave encounter angle is depicted in Figure 17, where the sign convention is that positive angles (unit pointing inwards for the port unit) are counted positive in clockwise direction by an observer situated on top of the unit.
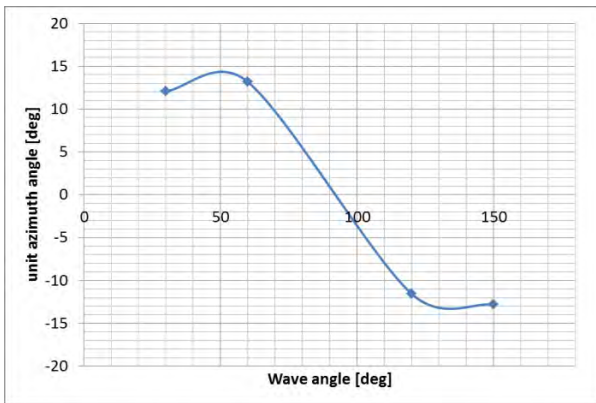
Figure 17 Typical azimuth angle when ventilation occurs for different waves encounter angles.

6 COMPARISON WITH FULL SCALE DATA

The tests which were performed in the ocean basin can be compared with the full scale data acquired during ship normal operation by the HeMoS which is installed on the ship. The HeMoS normally operates at 0.5 Hz, but the sampling frequency can be increased. For a period of some months the system was run at 5 Hz in order to provide higher resolution data. During this period many ventilation events were recorded, which were identified using the method described in Savio and Steen (2012). Among the retrieved events a group was recorded in condition similar to those tested in the ocean basin. According to the wave direction prediction archive of the European Centre for Medium-Range Weather Forecasts (ECMWF) and the ship heading the events were recorded in bow quartering condition. Figure 18 reports one of the events of the above mentioned group. The assumption of the event to have occurred in bow quartering seas is also supported by the fact that the local maximum of the submergence index happens almost at the same time as the minimum torque coefficient. The events recorded on that particular period of time tend to have very similar statistics showing that there is a strong correlation between sea state, wave encounter angle and ventilation events. Since it was argued that these events probably happened in bow quartering seas their statistics can be compared for instance to the 30 or 60 degrees events recorded in model scale.
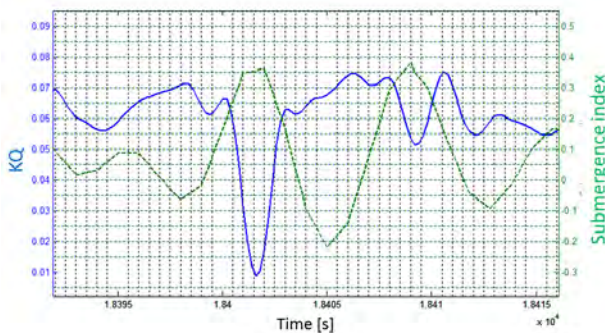

Figure 18 Sample of results from full scale measuremens by HeMoS in bow-quartering seas, showing the phasing between propeller submergence index and torque during a bow quartering event.

Table 3 Comparison of sample full scale results with model test results.

Param.	Full scale	Fr scaled to model sc.	Model sc. measured	Unit
T drop	1.2	0.3	0.21	[s]
dKq/dt	-0.037	-0.148	-0.77/-0.96	[1/s]
dKq	-0.044	-0.044	-0.021/-0.016	[]

Table 3 shows parameters extracted from the average full recorded time elapse of Figure 18 from the start of the event to the time of the minimum torque coefficient (T drop). The decrease rate during the events (dKq/dt) and torque drop (dKq) are reported in the second column. The corresponding model scale values according to Froude scaling and the recorded model scale values are reported in the third and fourth columns respectively. From the comparison of the values it is clear that the events in model scale are less violent than they should be from pure Froude scaling. This last fact confirms what is already pointed out by Califano in his doctoral thesis about the effect of air compressibility (Califano 2010). The effect of the air compressibility is to make ventilation stronger, since the air undergoes an expansion when it is drawn from the surface to the propeller. In model scale, the air is effectively incompressible, so there is almost no expansion, while in full scale the effect of compressibility is important. This could explain why the model scale events are less strong than what the simple Froude scaling predicts.

Regarding the model scale tests it was pointed out in the previous section that the autopilot could have had an influence on the results. From the analysis of the full scale data it can be seen that also other parts of the automation system of the ship should be included when undertaking ventilation studies. In Figure 19 and Figure 20 two different ventilation events are reported. The time series of the torque coefficient and its derivative are similar. However the time series of the shaft speed are rather dissimilar.
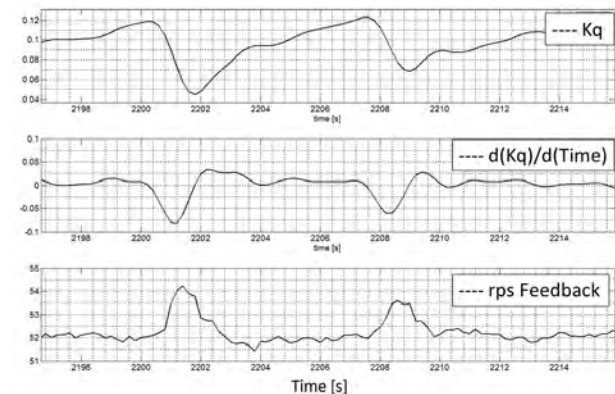

Figure 19 A recorded full scale event where the control system seems not to react to the torque drop.
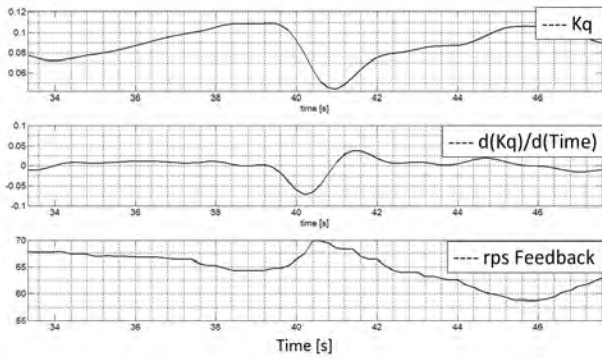
Figure 20 A recorded full scale event to which the control system reacted.

Both events show a clear propeller racing event in which the propeller revolutions increased about 2%. However in the event in Figure 19 the shaft speed returns to the pre-event speed rapidly after the event. On the contrary in the event depicted in Figure 20 the propeller revolutions are gradually reduced over a period of some seconds, before gradually returning to the pre-event value. The difference in the shaft speed time series can be a consequence of the different behavior of the control system during the two events. In the first case the control system did not react or if it reacted the effect is not clearly visible. In the second case the control system reacted and reduced the propeller speed. Although the control system is designed to protect the propulsive system in general it is currently not specifically designed to handle ventilation events. As pointed out by Smogeli et al (2009) the reaction of the controller to a ventilation event can be wrong, leading to damages to the propulsive system.

7 CONCLUSIONS

In the present paper some results of experiments carried out within the framework of the Era-Net Martec project PropSeas. From the model scale data it was demonstrated that ventilation doesn't seem to produce large overloads as is sometimes suggested, at least in model scale. However it was shown that the blade forces can undergo very large fluctuation due to the large in plane flow a propeller operating on an azimuthing thruster unit experiences during ship maneuvering. These large blade force variations pose the question if for instance also cavitation should be taken into account when studying dynamic forces on propellers in rough-water operation. Finally it is remarked that the problem of unit in service failures should be undertaken in an interdisciplinary way

including also for instance the propulsive control system or more in general the entire response of a ship to bad weather conditions.

LIST OF SYMBOLS

D= Propeller diameter [m]

R = propeller radius

h = distance from the propeller shaft to the water free surface

n , rps = Propeller speed [1/s]

V = Model speed [m/s]

T = Blade thrust [N]

Q = Propeller torque [Nm]

P = pressure measured on the hull in correspondence of the propeller disk [Pa]

fp = forward perpendicular

ap = aft perpendicular

$J = \dfrac{V}{nD}$ free stream advance coefficient

$Kt = \dfrac{T}{\rho n^2 D^4}$ Thrust coefficient

$Kq = \dfrac{Q}{\rho n^2 D^5}$ Torque coefficient

$Kp = \dfrac{P}{\rho n^2 D^2}$ Pressure coefficient

REFERENCES

Califano, Andrea (2010); "Dynamic loads on marine propellers due to intermittent ventilation" Doctoral theses at NTNU, ISSN 1503-8181; 2010:252

Koushan, K; (2006) "Dynamics of ventilated propeller blade loading on thrusters due to forced sinusoidal heave motion" Proceedings of 26th Symposium on Naval Hydrodynamics, ISBN-13: 978-0-9798095-0-7, Rome, Italy

Koushan, K.; Spence, S.J.B.; Hamstad, T. (2009) "Experimental Investigation of the Effect of Waves and Ventilation on Thruster Loadings" Proceedings of First International Symposium on Marine Propulsors, smp'09, ISBN 978-82-7174-263-8, Trondheim, Norway

Savio L., Steen S. (2012) "Identification and Analysis of Full Scale Ventilation Events," International Journal of Rotating Machinery, vol. 2012, Article ID 951642, 19 pages, 2012. doi:10.1155/2012/951642.

Smogeli, Øyvind Notland; Sørensen, Asgeir Johan, (2009) "Antispin Thruster Control for Ships". IEEE Transactions on Control Systems Technology 2009 ; Volume 17.(6) p. 1362-1375